# Three level signal transduction cascades lead to reliably timed switches

Dieter Armbruster[a], John Nagy[a,1], Jon Young[a]

[a] *Arizona State University*
[b] *Scottsdale Community College*

**Abstract**

Signaling cascades proliferate signals received on the cell membrane to the nucleus. While noise filtering, ultra-sensitive switches, and signal amplification have all been shown to be features of such signaling cascades, it is not understood why cascades typically show three or four layers. Using singular perturbation theory, Michaelis-Menten type equations are derived for open enzymatic systems. Cascading these equations we demonstrate that the output signal as a function of time becomes sigmoidal with the addition of more layers. Furthermore, it is shown that the activation time will speed up to a point, after which more layers become superfluous. It is shown that three layers create a reliable sigmoidal response progress curve from a wide variety of time-dependent signaling inputs arriving at the cell membrane, suggesting the evolutionary benefit of the observed cascades.

*Key words:* MAP-kinase network, Michaelis-Menten equations, time-dependent ODEs

## 1. Significance

In MAP-kinase signaling networks, three-level cascades are a very common motif. We try to understand why evolution would favor such a motif by analyzing the set of differential equations describing such signaling cascades. Specifically we study how such multi-level cascades process different time dependent input signals. Using a perturbation theory approach we find that the three level cascade architecture turns many different types of input signals into the

same sigmoidal output signal. Adding additional layers in the cascade does not change the type of output signal but delays its activation time.

## 2. Introduction

Biochemical cascades, in which upstream reaction products catalyze downstream reactions, are common patterns in eukaryotic molecular pathways. The mitogen-activated protein kinase (MAPK) system is an ancient, highly conserved example [1]. Functional and evolutionary studies of such cascades tend to emphasize their role as amplifiers of some input signal. Koshland et al. [2] (see also [3]) observe that "amplification" in this context involves at least two distinct notions: amplification of the absolute size of the signal and amplification of the change in signal intensity relative to the signal background intensity, so-called "fold" amplification [4]. Classic examples of the former include blood clotting [5, 6, 7, 8] and complement [9, 10] among others probably evolved from the same ancestral serine protease cascade [11]. The latter fold-change amplification is characteristic of signal transduction, at least for the MAPK and Wnt, $\beta$-catenin pathways [12, 13]. In both general cases, amplification is generated by layering in the cascade. Layering can also produce ultrasensitive responses, in which smooth changes in input are converted to a switch-like "off-on" output with a steeper signal-to-response curve than seen with traditional Michaelis-Menten dynamics [14, 15, 16, 2, 17, 3].

The intrinsic blood clotting mechanism of mammals was among the first biochemical cascades studied. Nearly simultaneously, Davie and Ratnof [6] and Macfarlane [8] proposed the same "waterfall" scheme of 8 reaction steps for this process, starting with factor XII activation and ending with conversion of fibrinogen (factor I) to fibrin. Macfarlane recognized immediately that such a cascade could amplify a small initiating signal into "an explosive generation of thrombin" and fibrin. Levine [7] studied the kinetics implied by Mcfarlane-Davie-Ratnof scheme by constructing a time-dependent mathematical model representing a simple linear cascade with no feedback. A unit pulse was intro-

duced at the first stage, and this signal propagated through $n$ stages. Levine defined the maximum gain of a stage—essentially the ratio of the steady state value of the $n^{\text{th}}$ stage versus the steady state value of the initial stage—and outlined how variations in duration of the initiating pulse affected signal dynamics of a 3-layered system.

More recently, signal transduction cascades have attracted a great deal of attention from theoreticians and modelers. In a signaling cascade, information in the form of a chemical cue received at the cell membrane propagates to transcription factors in the nucleus via a sequence of chemical reactions. The MAPK cascades represent the canonical examples. These systems are ubiquitous in eukaryotic organisms and regulate a variety of both normal and pathological cellular processes, including differentiation, proliferation, apoptosis and carcinogenesis [18, 1, 19]. Like the blood clotting cascade, signaling cascades comprise a number of layers, and MAP-kinase cascades are typically limited to 3 or sometimes 4 [18, pg. 102],[20]. Examples include a variety of mitogen-activated protein (MAP) kinase pathways—e.g., via extracellular signal-related kinases (ERKs), Jun amino-terminal kinases (JNKs) or p38 proteins [21, 22, 23]—phosphatidylinositol-3-kinase (PI3K) signaling via serine/threonine-specific kinase (Akt) and mammalian target of rifamycin (mTOR) [23, 24], Wnt signalling acting on $\beta$-catenin via the receptor Frizzled (Fz), Axin, glycogen synthase kinase 3 (GSK3) and other proteins [25], and the Janus kinase/Signal transducer and activator of transcription (Jak/Stat) pathway [23], among many others. In 2007, Coulombe and Meloche investigated atypical MAP-kinase cascades, ancient outliers that do not share the common characteristics of typical 3-tiered MAP-kinase cascades [20].

Why some signal transduction systems evolved into cascades remains an open question. One possibility is that cascades are one of Darwin's [26] predicted "imperfections"—the systems appear over-engineered and jury-rigged because they are cobbled together from parts that evolved originally for other purposes [27, pg. 104]. On the other hand, a number of alternative hypotheses have been proposed based on the dynamical properties of tiered cascades. Among the first

was a study by Huang and Ferrell [28], who extended an earlier mathematical model of Goldbeter and Koshland [15] to represent a 3-layered MAPK cascade in which double phosphorylation and dephosphorylation (activation and deactivation) of kinases were viewed as a single enzymatic reaction. They assumed a closed system and mass action kinetics and studied the equilibrium behavior of the resulting high-dimensional system of ordinary differential equations. They discovered that multiple layering generates an ultrasensitive signal-to-response curve, allowing cascades to behave like cooperative enzymes. Qiao et al. [29] expanded on this work by sampling a wider range of parameter values and discovered bistability and oscillations in the Huang-Ferrell model.

Ventura et al. [30] returned to the seminal work of Goldbeter and Koshland [15] with a more mechanistic eye. They modeled essentially the closed system of Figure 1, but approached the problem trying to understand how concentrations of species within the cascade impose dynamical constraints. Using the quasi-steady state assumption, they derived a one parameter equation for each layer, or module, of the cascade, representing one cycle of covalent modification. They then modeled an entire signaling cascade by linking together a sequence of these one parameter modules. Like Huang and Ferrell [28], they found ultrasensitive behavior in their model. They also discover damped oscillations in both their approximation of Figure 1. More importantly, they consider the case where the system is in a steady-state and one of the parameters is perturbed. They show that this information gets propagated both up and down the chain, which suggests that multiple layers in the cascade structure can facilitate cross-talk between networks without the need of explicit feedback loops.

Also digging into the details, Gomez-Uribe et al. [31] analyzed the functional repertoire of the phosphorylation-dephosphorylation reactions comprising a single layer of a cascade. They discovered that a single cycle can exhibit 4 steady-state response regimes. By appealing to the total quasi-steady-state assumption [32], they reduced their mass-action system into a single ordinary differential equation for the activated protein and used this approximation to study the system's response to sinusoidal input. They found that a single cycle acts as a

low-pass filter. Signaling pathways acting as low-pass filters was verified experimentally by Fujita *et al* in [33]. Any combination of these various dynamical behaviors—ultrasensitivity, bistability, oscillations, filtering and whole-system crosstalk—could be drivers of natural selection in signal transduction.

Here we suggest additional characteristics of multistage cascades that may be targets of selection. Our approach is unique in that we consider time-dependent inputs to both enzymatic "waterfalls," like blood clotting, and signal transduction cascades. Starting with signal transduction (Section 3.1) and moving to enzyme cascades (Section 3.2), we explore numerically the dynamics of various layers in response to a variety of time-varying inputs. Our explorations suggest that layers deep in the cascade exhibit time dependent switching behavior that is robust in the face of a wide range of time-dependent input functions. We then analyze the enzyme cascade using a perturbation analysis which reduces the system to a chain of one parameter modules, allowing us to establish a Michaelis-Menten type equation for open enzymatic systems (Section 3.3.1). Using this approximation, we validate our hypothesis that a sigmoidal time dependent output is a robust characteristic of 3- and 4-layer cascades for a very large class of temporally varying inputs. Extensive numerical simulations and intuition based on theoretical arguments point to the statement that a 4-stage cascade will guarantee a robust sigmoidal output for an arbitrary continuous input function. However, we are not able to prove this rigorously but relate the statement to an unproven open conjecture in probability theory and convex analysis. In addition, we also show the following: i) multiple layers filter out noise even without a deactivating enzyme;. ii) additional layers decrease the time it takes for the output to pass a threshold in cascades with identical modules; and iii) more than three or four layers causes a significant delay in activation time of the ultimate signal.

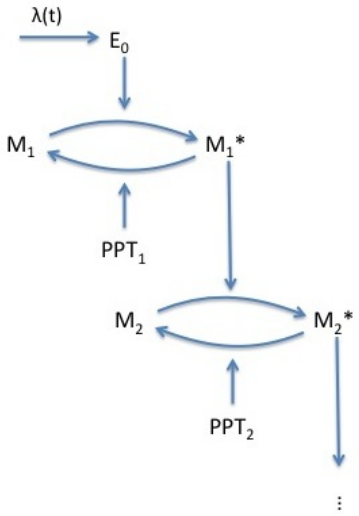


Figure 1: A basic signaling cascade.

## 3. Models

### *3.1. A Signaling Cascade with Opposing Covalent Modifications*

Although this paper is interested in a general model, the nomenclature for MAP-kinase cascades will be used here. In a basic signaling cascade, a protein gets modified by a kinase into an activated form. This activated protein then acts as the kinase for the next layer in the cascade. A phosphatase converts the activated form of the protein back into its inactive form. This study is interested in the dynamic response of the output signal with respect to a time-dependent input signal. In Figure 1, there is a flux of initial kinases at the top layer. The

stoichiometry for the basic signaling cascade is:

$$
\begin{aligned}
\varnothing &\xrightarrow{\lambda(t;\mu)} E_0 \\
E_0 + M_1 &\underset{d_1}{\overset{a_1}{\rightleftarrows}} C_1 \xrightarrow{k_1} E_0 + M_1^* \\
PPT_1 + M_1^* &\underset{\tilde{d}_1}{\overset{\tilde{a}_1}{\rightleftarrows}} X_1 \xrightarrow{\tilde{k}_1} PPT_1 + M_1 \\
M_1^* + M_2 &\underset{d_2}{\overset{a_2}{\rightleftarrows}} C_2 \xrightarrow{k_2} M_1^* + M_2^* \\
PPT_2 + M_2^* &\underset{\tilde{d}_2}{\overset{\tilde{a}_2}{\rightleftarrows}} X_2 \xrightarrow{\tilde{k}_2} PPT_2 + M_2 \\
&\vdots
\end{aligned}
\tag{1}
$$

where for every level $i$, the variables $M_i, M_i^*, C_i, PPT_i, X_i$ denote the protein, its activated form, the intermediate complex between the kinase and the protein it acts on, the phosphatase and the intermediate complex between the phosphatase and the protein it acts on, respectively. We call $E_0$ the initial kinase that flows into and out of the system at a rate of $\lambda(t;\mu)$ where $\mu$ is just a general set of parameters. $a_i$, $k_i$, $d_i$, $\tilde{a}_i$, $\tilde{k}_i$, and $\tilde{d}_i$ are the reaction rates. A mass-action model can be constructed to study the dynamical properties of the cascade structure.

For an $n$-layered cascade,

$$\begin{aligned}
\dot{M}_1 &= -a_1(\bar{\Lambda}(t;\mu) - C_1)M_1 + d_1C_1 + \tilde{k}_1X_1,\\
\dot{C}_1 &= a_1(\bar{\Lambda}(t;\mu) - C_1)M_1 - (d_1 + k_1)C_1,\\
\dot{M}_1^* &= k_1C_1 - \tilde{a}_1PPT_1M_1^* + \tilde{d}_1X_1\\
&\quad - a_2M_1^*M_2 + (d_2 + k_2)C_2\\
P\dot{P}T_1 &= -\tilde{a}_1PPT_1M_1^* + (\tilde{d}_1 + \tilde{k}_1)X_1,\\
\dot{X}_1 &= \tilde{a}_1PPT_1M_1^* - (\tilde{d}_1 + \tilde{k}_1)X_1,\\
&\vdots\\
\dot{M}_n &= -a_nM_n^*M_n + d_nC_n + \tilde{k}_nX_n,\\
\dot{C}_n &= a_nM_n^*M_n - (d_n + k_n)C_n,\\
\dot{M}_n^* &= k_nC_n - \tilde{a}_nPPT_nM_n^* + \tilde{d}_nX_n\\
P\dot{P}T_n &= -\tilde{a}_nPPT_nM_n^* + (\tilde{d}_n + \tilde{k}_n)X_n,\\
\dot{X}_n &= \tilde{a}_nPPT_nM_n^* - (\tilde{d}_n + \tilde{k}_n)X_n,
\end{aligned} \tag{2}$$

$$\begin{aligned}
&\bar{\Lambda}(0;\mu) = M_i^*(0) = C_i(0) = X_i(0) = 0,\\
&M_i(0) = \bar{M}_i, \text{ and } PPT_i(0) = \overline{PPT}_i \text{ for } 1 \le i \le n.
\end{aligned}$$

In (2),

$$\bar{\Lambda}(t;\mu) := E_0(t) + C_1(t) = \int_0^t \lambda(x;\mu)dx, \tag{3}$$

which is the total initial kinase concentration, and $\bar{\Lambda}$ is regarded as the input signal. The initial conditions reflect the case where no reaction has yet taken place, and no reaction will take place until $\bar{\Lambda}$ is positive.

The following assumptions about $\bar{\Lambda}$ reflect chemistry and experimental setups: Since $\bar{\Lambda}$ is a concentration, it is a continuous and non-negative function of time. Without a loss of generality, $\bar{\Lambda}(t,\mu)$ is positive for some interval $(0,\delta_0]$. The integral of $\bar{\Lambda}$ as time goes to infinity will be infinite reflecting the two typical examples where kinases are pumped into the system with no mechanism to escape, or a flux that is periodic. In addition, since the total number of

molecules is finite, $\bar{\Lambda}$ is bounded. Let $\bar{E}$ be the supremum of $\bar{\Lambda}$ and use it to define the scaled, total kinase concentration.

$$\Lambda = \bar{\Lambda}/\bar{E}.$$

To summarize, there exists a $\delta_0 > 0$ such that

$$\begin{aligned}
&\Lambda(t;\mu) \in C^0([0,\infty)),\\
&\Lambda(t;\mu) \geq 0,\\
&\sup_{[0,\infty)} \{\Lambda(t;\mu)\} = 1,\\
&\Lambda(0;\mu) = 0,\\
&\Lambda(t;\mu) > 0, \text{for all } 0 < t \leq \delta_0,\\
&\int_0^\infty \Lambda(x;\mu)dx = \infty.
\end{aligned} \tag{4}$$

*3.2. Enzymatic Cascade Model*

The parameters listed in [29] assume that the phosphatase concentrations are much lower than the proteins they act on. This is also argued in [30]. Taking this to the limit suggests looking at an enzymatic cascade model with no phosphatase, and seeing if the same type of behavior is observed.

Hence, for this basic model of an enzymatic cascade, the product of one reaction serves as the enzyme in the next reaction without a backward reaction to an inactivated enzyme. The total-enzyme concentration at the initial layer represents the time-dependent, input signal. For an $n$-stage cascade, the concentration of the final product, $P_n$, is considered the output signal. The

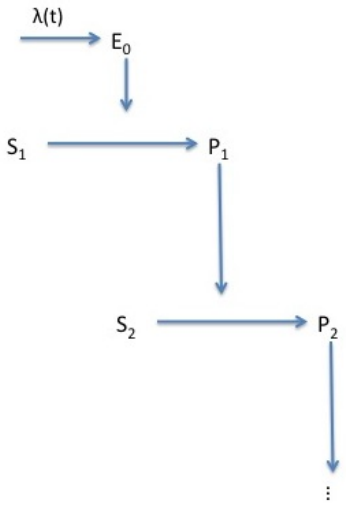


Figure 2: A basic enzymatic cascade.

stoichiometry is similar to Eq. (1):

$$
\begin{aligned}
\varnothing &\xrightarrow{\lambda(t;\mu)} E_0 \\
E_0 + S_1 &\underset{d_1}{\overset{a_1}{\rightleftarrows}} C_1 \xrightarrow{k_1} E_0 + P_1 \\
P_1 + S_2 &\underset{d_2}{\overset{a_2}{\rightleftarrows}} C_2 \xrightarrow{k_2} P_1 + P_2 \\
P_2 + S_3 &\underset{d_3}{\overset{a_3}{\rightleftarrows}} C_3 \xrightarrow{k_3} P_2 + P_3 \\
&\vdots
\end{aligned}
\tag{5}
$$

where $S, P, C$ are the substrates, product and the intermediate complex, respectively at each level and $E_0$ is the initial enzyme that flows into the system. A

mass-action model for an $n$-layered cascade is given by

$$\begin{aligned}
\dot{S}_1 &= -a_1(\bar{\Lambda}(t;\mu) - C_1)S_1 + d_1C_1, \\
\dot{C}_1 &= a_1(\bar{\Lambda}(t;\mu) - C_1)S_1 - (d_1 + k_1)C_1, \\
\dot{P}_1 &= k_1C_1 - a_2P_1S_2 + (d_2 + k_2)C_2, \\
&\vdots \\
\dot{S}_n &= -a_nP_{n-1}S_n + d_nC_n, \\
\dot{C}_n &= a_nP_{n-1}S_n - (d_n + k_n)C_n, \\
\dot{P}_n &= k_nC_n,
\end{aligned} \tag{6}$$

$$\begin{aligned}
\bar{\Lambda}(0;\mu) = P_i(0) = C_i(0) = 0 \text{ and} \\
S_i(0) = \bar{S}_i \text{ for } 1 \leq i \leq n.
\end{aligned}$$

The initial conditions reflect the case where no reaction has yet taken place and there are initial concentrations of substrates waiting for the influx of enzymes to start the chain reaction. $\bar{\Lambda}$ is defined in (3) and satisfies (4).

### *3.3. Approximating the Enzymatic Cascade*

#### *3.3.1. Singular Perturbation Theory*

We will express the enzymatic cascade model as a sequence of identical function operations. We will generate an operator relating input and output of a module, parametrized by a single parameter using perturbation techniques. In previous works such as [30], the authors used perturbation techniques to reduce the order of the set of ordinary differential equations, whereas this work aims to describe a cascade simply as an input/output functional operator.

The fundamental building block is a basic enzyme-substrate reaction:

$$\begin{aligned}
\varnothing &\xrightarrow{\lambda(t;\mu)} E \\
E + S &\underset{d_1}{\overset{a_1}{\rightleftarrows}} C \xrightarrow{k_1} E + P
\end{aligned} \tag{7}$$

Following the approach by Segel and others [34, 32, 35], who examined a system that is closed in the sense that there is no flux of molecules into or out of the system, we will derive a single, algebraic expression for the scaled product in the open system where the initial enzymes can flow into or out of the system. The following set of equations models the reaction (7):

$$\begin{aligned} E + C = \bar{\Lambda}(t;\mu) &= \int_0^t \lambda(x;\mu)dx, \\ S + C &= S_c, \\ \dot{S}_c &= -k_1 C, \\ \dot{C} &= a_1(\bar{\Lambda}(t;\mu) - C)(S_c - C) - (d_1 + k_1)C, \\ S_c(0) = \bar{S}, &\quad C(0) = 0, \end{aligned} \tag{8}$$

where $S_c$ is the total substrate concentration. In order to non-dimensionalize these equations we are going to scale the dependent variables by their suprema. It can be argued physically or by analyzing (8) that $C$ has a maximum. To get an estimate for the maximum of $C$, we set $\dot{C}$ equal to zero and determine a time $t_0$ such that

$$C_{max} = \frac{\bar{\Lambda}(t_0;\mu)S(t_0)}{K_m + S(t_0)} \leq \frac{\bar{E}\bar{S}}{K_m + \bar{S}} = \bar{C}.$$

Here $\bar{E}$ is the supremum of $\bar{\Lambda}$, and $K_m = (k_1 + d_1)/a_1$ is the Michaelis-Menten constant. The timescale for the total substrate depletion, as characterized in [36], can be estimated by:

$$t_{Sc} = (S_{c_{max}} - S_{c_{min}})/\left|\dot{S}_c\right|_{max} \approx \bar{S}/\left|k_1\bar{C}\right| = \frac{K_m + \bar{S}}{k_1\bar{E}}.$$

Defining the dimensionless variables

$$T = \frac{t}{t_{Sc}}, \quad s_c(T) = \frac{S_c(t)}{\bar{S}}, \quad c(T) = \frac{C(t)}{\bar{C}}, \quad \Lambda(T) = \frac{\bar{\Lambda}(t)}{\bar{E}},$$

and using the dimensionless parameters:

$$\sigma = \frac{\bar{S}}{K_m}, \quad \kappa = \frac{d_1}{k_1}, \quad \epsilon = \frac{\bar{E}}{K_m + \bar{S}},$$

the scaled dimensionless system of Equations (8) becomes:

$$\begin{aligned} s_c'(T) &= -c, \\ \epsilon c'(T) &= (\kappa+1)\left[((\sigma+1)\Lambda(T;\mu) - \sigma c)(s_c - \epsilon c) - c\right], \\ s(0) &= 1, \quad c(0) = 0. \end{aligned}$$

We now take the limit of $\epsilon$ to an arbitrarily small parameter ( $\epsilon \ll 1$) and expand $s_c$ and $c$ in powers of $\epsilon$ so that perturbation techniques can be used.

$$\begin{aligned} s_c(T) &\sim s_{c_0}(T) + \epsilon s_{c_1}(T) + \cdots, \\ c(T) &\sim c_0(T) + \epsilon c_1(T) + \cdots, \end{aligned}$$

Then the $O(1)$ equations are:

$$\begin{aligned} s_{c_0}' &= -c_0, \\ c_0 &= \frac{(\sigma+1)\Lambda(T;\mu)\, s_{c0}}{\sigma s_{c0} + 1}, \\ s_{c_0}(0) &= 1, \quad c_0(0) = 0, \end{aligned} \tag{9}$$

which can be solved for explicitly as

$$s_{c_0} = \frac{1}{\sigma} W\left[\sigma \exp\left(\sigma - (1+\sigma)\int_0^T \Lambda(x;\mu)dx\right)\right]$$

where $W$ is the Lambert-W function. If $p = P/\bar{S}$ is the scaled product, then

$$\begin{aligned} p(t) \approx p_0(T) &= F(\Lambda;\sigma) \equiv 1 - s_{c_0} \\ &= 1 - \frac{1}{\sigma} W\left[\sigma \exp\left(\sigma - (1+\sigma)\int_0^T \Lambda(x;\mu)dx\right)\right]. \end{aligned} \tag{10}$$

It should also be noted that by unscaling (14), one gets

$$\dot{S}_c = \frac{-V_{max}\Lambda S_c}{K_m + S_c},$$

where $V_{max} = k_1\bar{E}$ is the maximum velocity at which $P$ can be formed. This suggests that Michaelis-Menten parameters derived from closed systems should be applicable to the open enzymatic system. We discuss the accuracy of this perturbation expansion in [37].

*3.3.2. Viewing the Cascade as an Iteration*

Assuming that the timescales are the same at each stage and that $\epsilon \ll 1$, then the functional operator $F$ in (10) allows us to approximate (5) as a series of function compositions

$$\Lambda \xrightarrow{F} p_1 \xrightarrow{F} p_2 \xrightarrow{F} p_3 \cdots \tag{11}$$

treating the cascade as an iteration of the operation $F$, i.e. $p_1 = F(\Lambda)$, $p_2 = F(p_1)$, and so on. Since each stage of the iteration is based on the perturbation expansion, repeated iterations will lead to an accumulation or errors, details of which are discussed in [37].

## 4. Results

We present three sets of simulation results for the basic signaling cascade (Fig. 1), the enzymatic cascade (Fig. 2) and the functional operator (Eq. 11), respectively. It is shown that the most basic cascade (the functional operator) fundamentally leads to the same output signal as the other two cases hence isolating the function of the cascade to its basic mechanism.

Figure 3 plots simulation outputs for a basic signaling cascade with identical modules for various inputs. The reaction rates and initial conditions for the modules used in this study were taken from the range listed in [29]. However, unlike in [29], we assume that all modules are identical, and let $\bar{E}$, the supremum of the enzymatic input, vary up to the same order of magnitude as $\bar{M}$, the maximum of the substrate concentration.

In the first row of Figure 3 various input signals $\bar{\Lambda}(t)$ are plotted. In column (a), a sharply increasing function is plotted, a periodic function in column (b), and a slowly increasing function in column (c). In the second row, the outputs for various $n$-layered cascades are shown. In columns (a) and (b), it takes 3 stages for an output signal to become a regular sigmoidal curve. With a slowly increasing input, it takes 6 layers. The last row shows that adding additional layers appears to only move the output signal to the right. After a certain

number of layers, additional layers only delay the activation time for the final output.

Figure 3 illustrates the main results of our study: i) Multiple layers in a cascade filter out a wide variety of input signal behavior into a sigmoidal output curve—sigmoidal in the sense that the curve is increasing, bounded, and has a unimodal derivative. The only pertinent information that gets transmitted in a given time interval are $\int_0^t \Lambda dx$ and $\max\{\bar{\Lambda}\}$. ii) Although the output of a multi-layered cascade can approach a steady-state faster by increasing the number of layers, eventually additional layers will cause a delay.

Simulating the basic enzymatic cascade, we observe in Figure 4 the behavior of the outputs turning sigmoidal after a few layers, and additional layers delaying the approach to a steady-state after a certain point. These results are almost identical to the behavior observed in Figure 3, which strongly suggests that the cascade structure is responsible for these phenomena and not the cycle of kinase/phosphatase reactions.

Finally, iterating $F$ with the same input functions as in Figures (3) and (4) we find qualitatively the same results, shown in Figure 5. Specifically we find that a sharply increasing input immediately leads to an output signal that is sigmoidal in time (row 2, column (a)), it takes three layers for the output to become sigmoidal for a periodic input (row 2, column (b)) and three layers for the output signal generated by a slow input to converge to a fixed sigmoidal shape (row 2, column (c)). Figure 5 row 3 shows that after a four layer cascade, the output signals all look the same, independent of the initial form of the input. If we define the inflection point of the sigmoidal output as the *switching time* we find that for signals that don't increase slowly, after four layers, each subsequent cascade layer shifts the switching time by the same amount.

In producing the results for Figure 5, each iteration assumed that $\sigma = 5/3$. However, the fact that the curves appear to become sigmoidal after 3 iterations doesn't appear to be dependent on that fact. With a sinusoidal input, an experiment was ran where $\sigma$ was sampled uniformly from $[0, 5]$ for each layer. In 1000 trials, every 3-layered cascade had a sigmoidal output curve.

*4.1. Properties of the Functional Operator*

Simulations suggest that analyzing the operator $F$ (Eq. (10)) may explain why the cascade structure creates a sigmoidal output curve and why the timing of the output switch moves to the right with additional levels of the cascade. Basic calculus can be used to show that $F(\Lambda)$ will be increasing and $F^2(\Lambda)$ will be strictly increasing. The following lemma can also be proven.

**Lemma**

*If the input function $\Lambda(T)$ is an increasing, log-concave function with the properties listed in* (4)*, then $F(\Lambda)$ will be sigmoidal in the sense that it will be smooth, bounded, increasing, and have a unimodal derivative.*

**Proof:**

From Eq. (14), it can be shown that:

$$\frac{c_0'}{c_0} = \frac{\Lambda'}{\Lambda} - \frac{(\sigma+1)\Lambda}{(\sigma s_{c_0}+1)^2}.$$

It is easy to show that based on Eq. (14), $s_{c_0}$ is a decreasing function. Since $\Lambda$ is assumed to be increasing, this implies $-\frac{(\sigma+1)\Lambda}{(\sigma s_{c_0}+1)^2}$ is decreasing. Since $\Lambda$ is assumed to be log-concave, $\frac{\Lambda'}{\Lambda}$ is decreasing. Therefore, $c_0$ is log-concave, and hence, unimodal. It is easy to show that $F(\Lambda) = p_0$ is smooth, bounded, and increasing. □

Interestingly, $p_0$ can be extended so that it defines a cumulative probability distribution with semi-infinite support. $c_0$ can be considered the probability density. This motivates the following conjecture in probability theory.

**Conjecture**: *Let $\Lambda$ be a continuous probability distribution with semi-infinite support and let $F(\Lambda)$ be defined as in Eq.* (10). Then there exists an $n \in \mathbb{N}$ such that $F^k(\Lambda)$ will be a probability distribution with a unimodal density for all $k \geq n$.

The form of $F$ from (10) suggests why the cascade structure acts as a time-dependent filter. To restate,

$$F(\Lambda) = 1 - \frac{1}{\sigma} W \left[ \sigma \exp\left( \sigma - (\sigma + 1) \int_0^T \Lambda(x) dx \right) \right].$$

Notice that since $F$ integrate the input signal over time, any input signal is smoothed. Defining

$$h(T) = 1 - \frac{1}{\sigma} W \left[ \sigma \exp\left( \sigma - (\sigma + 1) T \right) \right], \tag{12}$$

it is straightforward to show that $h$ is strictly increasing and concave by looking at the properties of $W$ from [38], or by starting from the ODE from which $h$ is derived. Hence, since $F(\Lambda) = h(\int_0^T \Lambda(x) dx)$, $F$ smoothes the input signal and composes it with a strictly increasing, concave function, which suggests why the outputs become sigmoidal.

While our simulations suggest that if $\Lambda$ satisfies (4), then $F^3(\Lambda)$ is sigmoidal, by carefully analyzing $F$, we find a (although biologically unlikely) counterexample to this statement: Figure 6 shows an input signal where $\Lambda(t)$ is a periodic sequence consisting of short and small trapezoidal signal followed by a delayed, large $\delta$-type impulse. The same figure shows the third layer output which is not sigmoidal since its derivative is not unimodal. However, the fourth layer output becomes sigmoidal.

## 5. Discussion

The derivation of Equation (10) allows us to model an enzymatic cascade as a sequence of function operators assuming that at each stage the timescales are the same and that $\epsilon \ll 1$. If these hypotheses are satisfied, an interesting theoretical backbone emerges as to function and structure of multiple enzymatic cascades.

Our approach looks at extensive simulations, understanding that they lack analytic rigor, in combination with the mathematical analysis of simpler, approximated models, understanding that these simpler models may not encapsulate every physically relevant situation—approximations and restrictions are

made when deriving these simpler models; however, the combination of both supports our hypotheses. We have observed through simulations some very interesting signal processing properties of a cascade architecture, and this may be because at their core, these cascades behave like the iteration of a functional operator that integrates the incoming signal, which smoothes it out, and then composes the result with a bounded monotonic function. The use of the functional operator is interesting because it allows tools from other disciplines, such as probability theory and convex analysis, to be used to try and answer questions regarding the behavior of enzymatic cascades.

We find that the cascade structure acts as a filter to transform a variety of persistent input signal types into a common sigmoidal response, and typically no more than 3 layers are required to produce this effect. For slowly increasing inputs, additional layers will speed up the time it takes for the product concentration to approach the steady-state. After a certain number of layers, typically after three, increasing the number of layers further will delay the time it takes for the final output to approach steady-state. To study the details of behavior, we investigated a drastically simplified enzymatic cascade showing the same phenomena.

Biologically, the cascade structure may have evolved in part because it creates a very reliable sigmoidal response robust to variations in input. In particular, cells must decipher noisy input signals using an enzymatic system that, due to promiscuous interactions among component proteins and other causes, itself generates noise [39, 40]. By organizing the signal into a cascade, the only information that gets transmitted in a given time interval is the total amount of enzymes in the system during that time interval — it doesn't matter if the total enzyme concentration is fluctuating or increasing. Therefore, the cascade structure generates a reliable switch, irrespectively of the way the total enzyme concentration arrives at the critical value. It seems for most practical purposes, a three layer cascade will do precisely this; therefore, adding more layers to the cascade serves no apparent purpose.

To understand why the output is indeed sigmoidal and that after a certain

point additional layers only delays the activation time, a functional operator was derived for an open enzymatic system based on perturbation techniques similar to the ones employed by [34] and [35]. This functional operator smoothes the signal by integrating and then composes the integral with a monotonically increasing concave function. This generates a novel conjecture in probability theory that we are unable to prove rigorously at this time.

An interesting consequence of our perturbation analysis is that if $\epsilon \ll 1$, then the steady-state parameters derived for a closed enzymatic system can be used when those systems are open networks embedded in a larger chemical reaction network. Such open networks have been discussed in Eq. (7) motivated by the need to modularize the enzymatic cascade. We show that it is possible to use Michaelis-Menten parameters when a module is embedded in a larger network. In addition, there are other open networks such as those with a flux of substrates [41] or networks with mechanisms that destroy enzymes where our results may apply.

As is often the case in perturbation arguments, if $\epsilon = O(1)$, the results may still hold: For the parameters listed in Table 1, $\epsilon \approx 0.6$ the simulations of the basic model and the functional iteration model are qualitatively correct and quantitatively close but not perfect. In [37] we discuss in detail the error behavior of the perturbation scheme and show that the errors between the full simulation and the perturbation scheme go to zero as $\epsilon \to 0$.

The fact that the simplified enzymatic cascade is based on the assumption that the phosphatase concentration is much smaller than the proteins they act on (true for signaling cascades) is important for the sigmoidal output signal: If the phosphatase concentration is allowed to be on the same order as their target molecules, then the filtering behavior of signaling cascades deteriorates dramatically. By using the same parameters as in Table 1, but with $\overline{PPT}_i = 0.5\mu M$, the oscillations from an input can persist much longer. Figure 7 shows the output for a 1-layer, 5-layer, and 10-layer cascade. Another issue with the simplified enzymatic cascade is the fact that that there is no mechanism to shut the system down. A small pulse, no matter how small or brief, is guaranteed

to activate a full response in an enzymatic cascade with more than one layer. Future work will focus on brief pulses which are likely to be subcritical and on the shut down behavior of signaling cascades.

Table 1: The parameters used for Figures 3, 4, and 5. $i \geq 1$ and $j > 1$.

| | | | |
|---|---|---|---|
| $a_i = \tilde{a}_i = 200 \quad (\mu M \cdot min)^{-1}$ | $\bar{E} = 0.1 \quad \mu M$ | $\epsilon_1 = 0.125$ | $\epsilon_j = 0.625$ |
| $k_i = \tilde{k}_i = 30 \quad min^{-1}$ | $\bar{S}_i = 0.5 \quad \mu M$ | $t_{sc_1} = 0.2667 \quad min$ | $t_{sc_j} = 0.0533 \quad min$ |
| $d_i = \tilde{d}_i = 30 \quad min^{-1}$ | $\overline{PPT}_i = 0.024 \quad \mu M$ | $\sigma_1 = 1.67$ | $\sigma_j = 1.67$ |

## 6. Appendix

This appendix presents some of the mathematical details of the singular perturbation theory for time dependent Michaelis Menten models. It follows closely the presentation in [37].

### *6.1. Accuracy of the Time-Dependent Approximation*

In our analysis, we do not invoke the quasi-steady state assumption because the complex concentration can fluctuate depending on the behavior of the input signal, $\bar{\Lambda}$. Also, unlike the work done on the closed system, the existence of a boundary layer is dependent on whether there is a boundary layer in the dynamics of $\bar{\Lambda}$. However, when the system is scaled on the time of the product formation and perturbation methods are invoked, the initial values for the $O(1)$ equations are the same as the system they are approximating. Discrepancies could arise, depending on $\bar{\Lambda}$, in the initial conditions when looking at the $O(\epsilon)$ equations. We would like to keep $\bar{\Lambda}$ as general as possible, and do our analysis on the time-scale of product formation, which is the same as looking at the total-substrate depletion, $S_c$.

To scale the dependent variables, it is necessary to get an estimate for their maximum values. Clearly, $S(0)$, which is labeled as $\bar{S}$, is the maximum of $S_c$, and by assumption $\bar{E}$ is the supremum of $\bar{\Lambda}$. It is not as easy to estimate the maximum of $C$ given the generality of $\bar{\Lambda}$. In all cases that would make physical

sense, $C$ has a global maximum. Let $t_0$ be the time at which the global max occurs. At this maximum, the derivative of $C$ will be zero, and an upper bound, $\bar{C}$, can be derived which will be used as an estimate for $C$.

$$C_{max} = \frac{\bar{\Lambda}(t_0)S(t_0)}{K_m + S(t_0)} \leq \frac{\bar{E}\bar{S}}{K_m + \bar{S}} = \bar{C}.$$

This estimate can then be used to derive an estimate for the maximum of $\left|\dot{S}_c\right|$ and an estimate for the time-scale of $S_c$. Since $\dot{S}_c = -k_1 C$,

$$t_{Sc} = (S_{c_{max}} - S_{c_{min}}) / \left|\dot{S}_c\right|_{max} \approx \bar{S} / \left|k_1 \bar{C}\right| = \frac{K_m + \bar{S}}{k_1 \bar{E}}.$$

Defining the dimensionless variables

$$T = \frac{t}{t_{Sc}}, \quad s_c(T) = \frac{S_c(t)}{\bar{S}}, \quad c(T) = \frac{C(t)}{\bar{C}}, \quad \Lambda(T) = \frac{\bar{\Lambda}(t)}{\bar{E}},$$

and using the dimensionless parameters:

$$\sigma = \frac{\bar{S}}{K_m}, \quad \kappa = \frac{d_1}{k_1}, \quad \epsilon = \frac{\bar{E}}{K_m + \bar{S}},$$

the dimensionless system is:

$$\begin{aligned} s_c' &= -c, \\ \epsilon c' &= (\kappa + 1)\left[((\sigma + 1)\Lambda - \sigma c)(s_c - \epsilon c) - c\right], \\ s_c(0) &= 1, \quad c(0) = 0. \end{aligned} \tag{13}$$

The $O(1)$ equations are:

$$\begin{aligned} c_0 &= \frac{(\sigma + 1)\Lambda s_{c_0}}{\sigma s_{c_0} + 1}, \\ s_{c_0}' &= -c_0. \end{aligned} \tag{14}$$

It should be useful to note that

$$c_0' = \frac{(\sigma + 1)s_{c_0}\Lambda'}{\sigma s_{c_0} + 1} + \frac{(\sigma + 1)s_{c_0}'\Lambda}{(\sigma s_{c_0} + 1)^2}.$$

The $O(\epsilon)$ equations are:

$$\begin{aligned} c_1 &= \frac{1}{1 + \sigma s_{c_0}}\left(c_0(\sigma c_0 - (\sigma + 1)\Lambda) + ((\sigma + 1)\Lambda - \sigma c_0)s_{c_1} - \frac{c_0'}{\kappa + 1}\right), \\ s_{c_1}' &= -c_1. \end{aligned}$$

The equation for $s_{c_1}$ can be expressed as:

$$s'_{c_1} = -P(T)s_{c_1} + Q(T),$$

where

$$\begin{aligned}
P(T) &= \frac{1}{1+\sigma s_{c_0}}((\sigma+1)\Lambda - \sigma c_0) = \frac{-s'_{c_0}}{s_{c_0}} + \frac{\sigma s'_{c_0}}{1+\sigma s_{c_0}}, \\
Q(T) &= \frac{1}{1+\sigma s_{c_0}}\left(\frac{c'_0}{\kappa+1} + c_0((\sigma+1)\Lambda - \sigma c_0)\right) \\
&= \frac{1}{1+\sigma s_{c_0}}\left(\frac{(\sigma+1)s_{c_0}\Lambda'}{(\kappa+1)(\sigma s_{c_0}+1)} + \frac{(\sigma+1)s'_{c_0}\Lambda}{(\kappa+1)(\sigma s_{c_0}+1)^2} - (\sigma+1)\Lambda s'_{c_0} + \frac{\sigma s'_{c_0}(\sigma+1)s_{c_0}\Lambda}{\sigma s_{c_0}+1}\right).
\end{aligned}$$

Hence, the integrating factor is:

$$\exp\left(\int_0^T P(x)dx\right) = \frac{1+\sigma s_{c_0}}{s_{c_0}}.$$

Hence,

$$\exp\left(\int_0^T P(x)dx\right)Q(T) = \frac{(\sigma+1)\Lambda'}{(\kappa+1)(\sigma s_{c_0}+1)} + (\sigma+1)\Lambda\left(\frac{s'_{c_0}}{(\kappa+1)s_{c_0}(\sigma s_{c_0}+1)^2} - \frac{s'_{c_0}}{s_{c_0}(\sigma s_{c_0}+1)}\right).$$

Let $u(y) = s_{c_0}(y)$ and $v(y) = \Lambda(y)$. Then

$$\left|\int_0^T \exp\left(\int_0^y P(x)dx\right)Q(y)dy\right| \le \frac{\sigma+1}{\kappa+1}\int_0^\Lambda dv + \frac{\sigma+1}{\kappa+1}\left|\int_{s_{c_0}}^1 \frac{1}{u(\sigma u+1)^2}du\right| + (\sigma+1)\left|\int_{s_{c_0}}^1 \frac{1}{u(\sigma u+1)}du\right|.$$

We are left with the inequality:

$$\begin{aligned}
|s_{c_1}| &\le \frac{(\sigma+1)s_{c_0}\Lambda}{(\sigma s_{c_0}+1)(\kappa+1)} + \frac{\sigma s_{c_0}(1-s_{c_0})}{(\kappa+1)(\sigma s_{c_0}+1)^2} - \frac{(\sigma+1)s_{c_0}}{(\kappa+1)(\sigma s_{c_0}+1)}\log\left(\frac{(\sigma+1)s_{c_0}}{\sigma s_{c_0}+1}\right) \\
&\quad - \frac{(\sigma+1)s_{c_0}}{\sigma s_{c_0}+1}\log\left(\frac{(\sigma+1)s_{c_0}}{\sigma s_{c_0}+1}\right) \\
&\le \frac{1}{\kappa+1}\left(2+\frac{1}{e}\right) + \frac{1}{e} < 3,
\end{aligned}$$

which implies that $s_{c_1}$ is bounded and hence the perturbation scheme is valid.

Figure 8 shows plots demonstrating the accuracy of the approximated solutions for $\sigma = 1$, $\kappa = 1$, $\epsilon = 0.1$ and $\Lambda_1 = 0$. Figure 8b shows that the $O(1)$ solution based on Equation (14) has a small error (approximately $O(\epsilon)$) relative to the actual solution calculated from Equation (13). Adding the solution based on the $O(\epsilon)$ expansion gives high accuracy as can be seen in Figure 8d.

*6.2. Accuracy of the Iteration Scheme*

Since $F$ is an $O(1)$ approximation to the true output, treating a cascade as an n-fold iteration of $F$ has the potential to introduce additional error. It is intuitive that one can trade the number of iterations against the smallness of $\epsilon$.

We can see how perturbations in the input would propagate through the approximated model. Suppose $\Lambda$ is the input and $\Lambda + \epsilon\Lambda_1$ is the perturbed input. Let $s_{c_0}$ be the output for $\Lambda$ and $\tilde{s}_{c_0}$ be the output to the perturbed input. Then

$$\log(s_{c_0}) + \sigma s_{c_0} = \sigma - (\sigma + 1) \int_0^T \Lambda(x)dx,$$
$$\log(\tilde{s}_{c_0}) + \sigma \tilde{s}_{c_0} = \sigma - (\sigma + 1) \int_0^T \Lambda(x) + \epsilon\Lambda_1(x)dx,$$

which implies

$$\log(s_{c_0}) - \log(\tilde{s}_{c_0}) + \sigma(s_{c_0} - \tilde{s}_{c_0}) = (\sigma + 1)\epsilon \int_0^T \Lambda_1(x)dx.$$

By the Mean Value Theorem, there exists $\xi \in (\tilde{s}_{c_0}, s_{c_0}) \subset (0, 1]$, such that

$$\log(s_{c_0}) - \log(\tilde{s}_{c_0}) = \frac{1}{\xi}(s_{c_0} - \tilde{s}_{c_0}).$$

This implies that

$$|s_{c_0} - \tilde{s}_{c_0}| = \left|\frac{\sigma + 1}{\sigma + 1/\xi}\right| \left|\epsilon \int_0^T \Lambda_1(x)dx\right| \leq \epsilon \left|\int_0^T \Lambda_1(x)dx\right|.$$

This suggests that using a sequence of function compositions as a model of a signaling cascade works well if $\left|\int_0^\infty s_1(x)dx\right|$ is bounded. Unfortunately, given the general properties of the input $\Lambda$, it can be shown that $\left|\int_0^\infty s_1(x)dx\right|$ can be made arbitrarily large and could quite possible be unbounded. It is possible to contrive counter-examples demonstrating a large error between the outputs with inputs that are $O(\epsilon)$ between each other, but for most relevant situations, the outputs tend to stay close to each other. More work is needed to determine exactly what additional properties of $\Lambda$ would guarantee close outputs.

Figure 9 shows examples of when $\epsilon = 0.1$ and when $\epsilon = 0.01$ for a 1-layer, 5-layer, and 10-layer cascade.

## Acknowledgments

This work was partially supported by More Graduate Education at Mountain States Alliance (MGE@MSA), Alliance for Graduate Education and the Professoriate (AGEP), National Science Foundation (NSF) Cooperative Agreement No. HRD-0450137 (to J.Y.) and by the Volkswagen Foundation under the program on Complex Networks (to D.A. and J.Y.).

## References

[1] W. Kolch, Meaningful relationships: The regulation of the RAS/Raf/MEK/ERK pathway by protein interactions, Biochemical Journal 351 (2000) 289–305.

[2] D. E. Koshland, A. Goldbeter, J. B. Stock, Amplification and adaptation in regulatory and sensory systems, Science 217 (1982) 220–225.

[3] Q. Zhang, S. Bhattacharya, M. E. Andersen, Ultrasensitive response motifs: Basic amplifiers in molecular signalling networks, Open Biology 3 (2013) 130031.

[4] J. E. Ferrell, Signaling motifs and Weber's law, Molecular Cell 36 (2009) 724–727.

[5] R. L. C. Adams, R. J. Bird, Review article: Coagulation cascade and therapeutics update: Relevance to nephrology. Part 1: Overview of coagulation, thrombophilias and history of anticoagulants, Nephrology 14 (2009) 462–470.

[6] E. W. Davie, O. D. Ratnoff, Waterfall sequence for intrinsic blood clotting, Science 145 (3638) (1964) 1310–1312.

[7] S. N. Levine, Enzyme amplifier kinetics, Science 152 (3722) (1966) 651–653.

[8] R. G. Macfarlane, An enzyme cascade in the blood clotting mechanism, and its function as a biochemical amplifier, Nature 202 (1964) 498–499.

[9] F. Forneris, J. Wu, P. Gros, The modular serine proteases of the complement cascade, Current Opinion in Structural Biology 22 (2012) 333–341.

[10] D. Ricklin, *et al*, Complement: A key system for immune surveillance and homeostasis, Nature Immunology 11 (2010) 785–797.

[11] M. M. Krem, E. Di Cera, Evolution of enzyme cascades from embryonic development to blood coagulation, Trends in Biochemical Sciences 27 (2002) 67–74.

[12] C. Cohen-Saidon, *et al*, Dynamics and variability of ERK2 response to EGF in individual living cells, Molecular Cell 36 (2009) 885–893.

[13] L. Goentoro, M. W. Kirschner, Evidence that fold-change, and not absolute level, of $\beta$-catenin dictates Wnt signaling, Molecular Cell 36 (2009) 872–884.

[14] J. E. Ferrell, Tripping the switch fantastic: How a protein kinase cascade can convert graded inputs into switch-like outputs, Trends in Biochemical Sciences 21 (1996) 460–466.

[15] A. Goldbeter, D. E. Koshland, An amplified sensitivity arising from covalent modification in biological systems, Proceedings of the National Academy of Sciences 78 (1981) 6840–6844.

[16] A. Goldbeter, D. E. Koshland, Ultrasensitivity in biochemical systems controlled by covalent modification: Interplay between zero-order and multistep effects, Journal of Biological Chemistry 259 (1984) 14441–14447.

[17] B. N. Kholodenko, Negative feedback and ultrasensitivity can bring about oscillations in the mitogen-activated protein kinase cascade, European Journal of Biochemistry 267 (2000) 1583–1588.

[18] E. Klipp, *et al*, Systems Biology, Wiley-VCH Verlg GmbH & Co. KGaA, Weinheim, 2009.

[19] J. A. McCubrey, *et al*, Roles of the raf/mek/erk pathway in cell growth, malignant transformation and drug resistance, Biochimica et Biophysica Acta 1773 (2007) 1263–1284.

[20] P. Coulombe, S. Meloche, Atypical mitogen-activated protein kinases: Structure, regulation and functions, Biochimica et Biophysica Acta-Molecular Cell Research 1773 (8) (2007) 1376–1387.

[21] L. Chang, M. Karin, Mammalian map kinase signalling cascades, Nature 410 (2001) 37–40.

[22] G. Sabio, J. Davis, Tnf and map kinase signalling pathways, Seminars in Immunology.
URL `http://dx.doi.org/10.1016/j.smim.2014.02.009`

[23] P. Trikha, W. E. C. III, Signaling pathways involved in mdsc regulation, Biochimica et Biophysica Acta 1846 (2014) 55–65.

[24] C. Porta, C. Paglino, A. Mosca, Targeting pi3k/akt/mtor signaling in cancer, Frontiers in Oncology 4 (2014) 1–11.

[25] H. Clevers, R. Nusse, Wnt/$\beta$-catenin signaling and disease, Cell 149 (2012) 1192–1205.

[26] C. Darwin, On the Origin of Species by Means of Natural Selection, or the Preservation of Favoured Races in the Struggle for Life, 1st Edition, John Murray, London, 1859.

[27] S. J. Gould, The Structure of Evolutionary Theory, Belnap Press, Cambridge, UK, 2002.

[28] C. Huang, J. Ferrell, Ultrasensitivity in the mitogen-activated protein kinase cascade, Proceedings of the National Academy of Sciences 93 (1996) 10078–10083.

[29] L. Qiao, *et al*, Bistability and oscillations in the huang-ferrell model of mapk signaling, PLoS Computational Biology 3 (9) (2007) 1819–1826.

[30] A. Ventura, J.-A. Sepulchre, S. Merjver, A hidden feedback in signaling cascades is revealed, PLoS Computational Biology 4 (3) (2007) 1–14. arXiv:e1000041.

[31] C. Gomez-Uribe, *et al*, Operating regimes of signaling cycles: Statics, dynamics, and noise filtering, PLoS Computational Biology 3 (12) (2007) 2487–2497.

[32] J. Borghans, *et al*, Extending the quasi-steady state approximation by changing variables, Bulletin of Mathematical Biology 58 (1996) 43–63.

[33] K. A. Fujita, *et al*, Decoupling of receptors and downstream signals in the akt pathway by its low-pass filter characteristics, Science Signaling 3 (132).

[34] L. A. Segel, M. Slemrod, The quasi-steady-state assumption: A case study in perturbation, SIAM Review 31 (3) (1989) 446–447.

[35] S. Schnell, C. Mendoza, A closed-form solution for time-dependent enzyme kinetics, Journal of Theoretical Biology 187 (1997) 207–212.

[36] C. C. Lin, L. A. Segel, Mathematics Applied to Deterministic Problems in Natural Sciences, Macmillan Publishing, 1974.

[37] J. Young, D. Armbruster, J. Nagy, Time-dependent michaelis-menten equations for open-enzyme networks, in: A. Mikhailov, G. Ertl (Eds.), Engineering of Chemical Complexity, Vol. II, World Scientific, Singapore, 2014.

[38] R. M. Corless, *et al*, On the lambertw function, Advances in Computational Mathematics 5 (1) (1996) 329–359.

[39] J. E. Ladbury, S. T. Arnold, Noise in cellular signalling pathways: Causes and effects, Trends in Biochemical Sciences 37 (2012) 173–178.

[40] C. Waltermann, E. Klipp, Information theory based approaches to cellular signaling, Biochimica et Biophysica Acta 1810 (2011) 924–932.

[41] I. Stoleriu, F. Davidson, J. Liu, Quasi-steady state assumptions for non-
460 isolated enzyme-catalysed reactions, Journal of Mathematical Biology 48 (2004) 82–104.

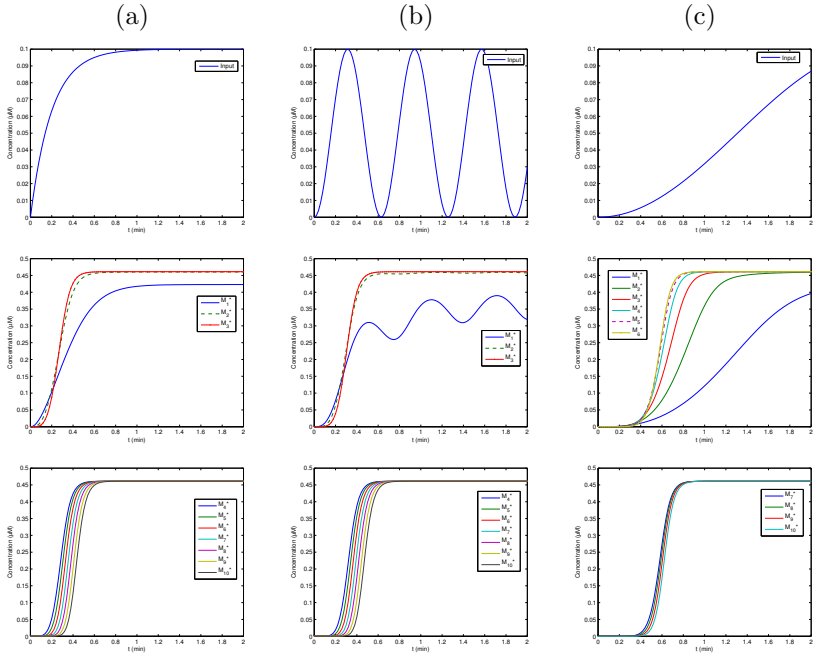


Figure 3: Plots of various inputs and their outputs for a basic signaling cascade with identical modules. In the first row, various input signals are plotted. $\bar{\Lambda}(t)$ is increasing fast in column (a), is periodic in column (b) and increases very slowly in column (c). In the second row, the outputs for various $n$-layered cascades are shown. We see that the point of inflection of the output signal *advances* (moves to the left) with additional cascade levels. The last row shows that adding additional layers beyond 4 (for column (a) and (b)) and seven (column (c)) only delays the rise of the output signal. The small amount of phosphatase in the system means that the signaling cascade will behave similarly to an enzymatic cascade, so multiple layers will smooth out an oscillating input.

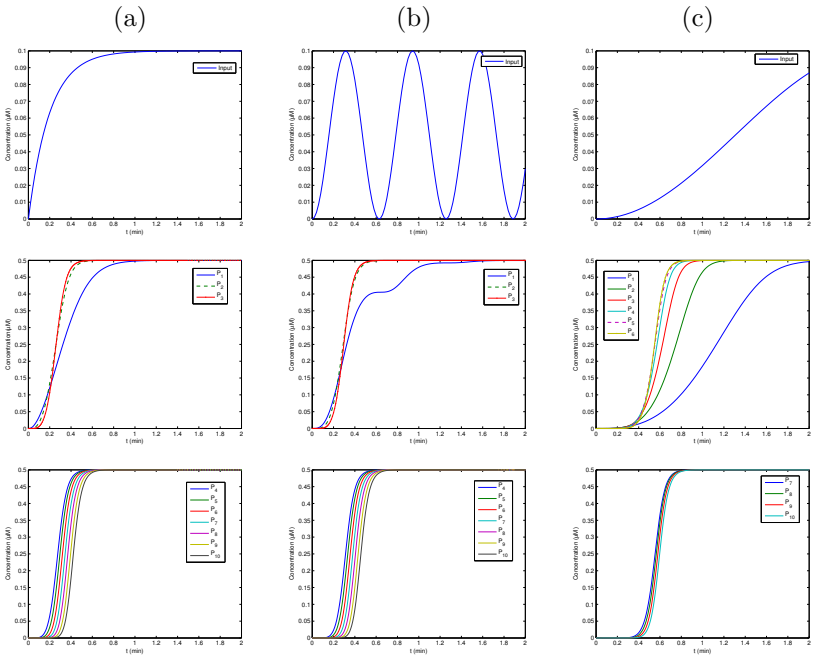


Figure 4: Plots of various inputs and their outputs for a basic enzymatic cascade with identical modules. The behavior of the outputs for the enzymatic cascade model is similar to that of the results for the signaling cascade model in Figure 3. One major difference is in the center graph. Unlike the signaling cascade with opposing covalent modifications, there is no mechanism for the product molecules to be deactivated. Hence, they are always increasing, but the effect of an oscillating input is still apparent.

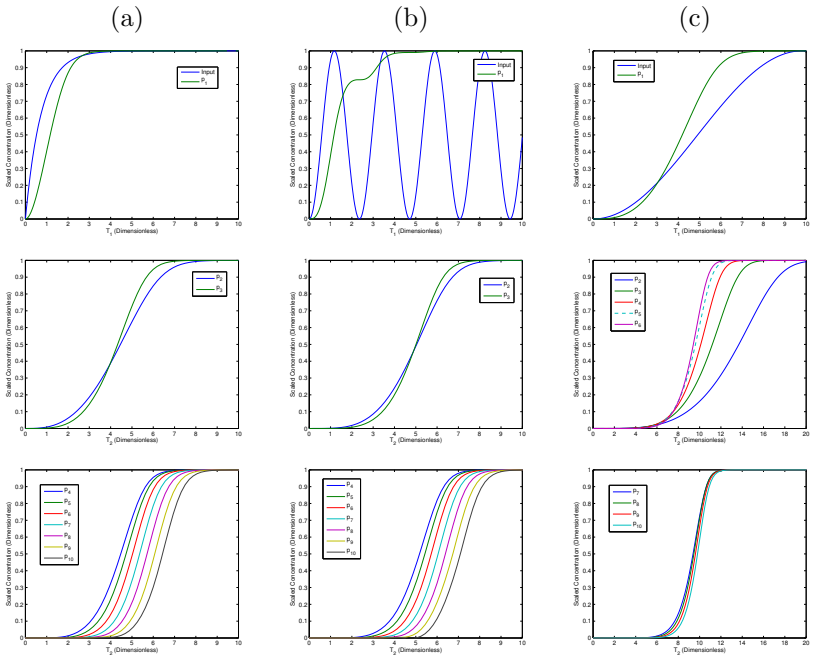


Figure 5: Plots of various inputs and their outputs for (11) model of an enzymatic cascade. As in Figures 3 and 4 the first row shows a sharply increasing input function (column (a)), a periodic input column (b)) and a slowly increasing input (column(c)). The outputs for these inputs for the first three cascades are shown in row two and the outputs for cascades four to ten is shown in row three. In all cases, it appears that the shift to the right becomes constant. The parameters used for these simulations can be found in Table 1.

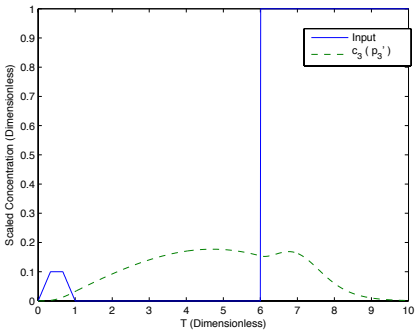


Figure 6: A 3rd layer output that is not sigmoidal.

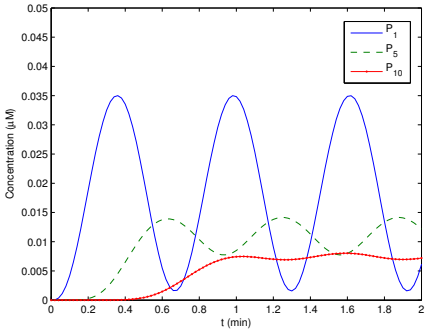


Figure 7: What happens when the phosphatase concentration is on the same order of its substrate.

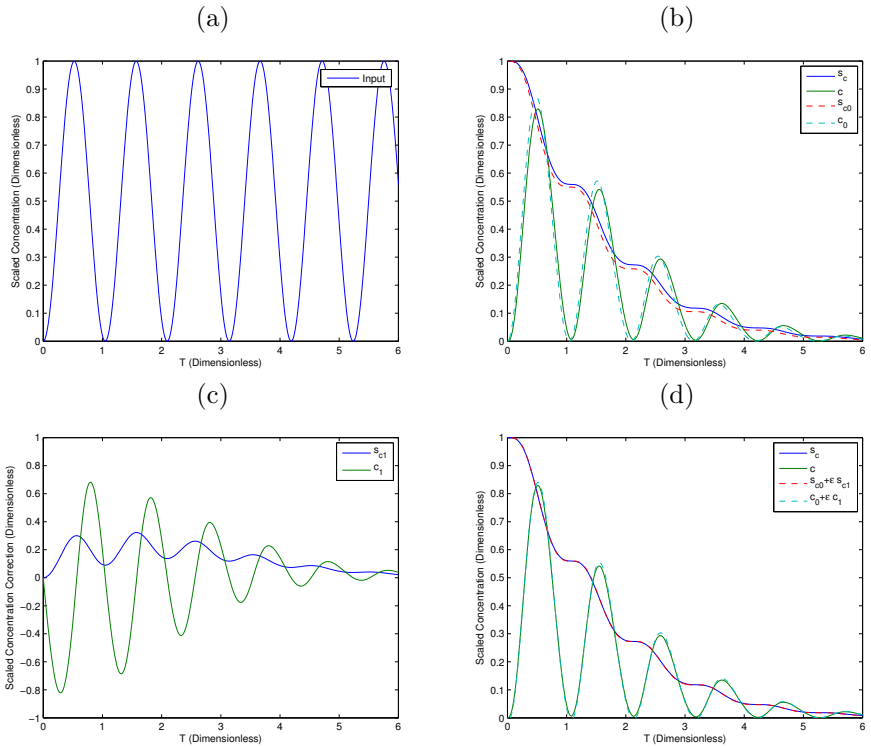


Figure 8: Plots demonstrating the accuracy of the perturbation expansion. (a) the input function $\Lambda_0$, (b) the exact solution and the $O(1)$ approximations, (c) the $O(\epsilon)$ correction and (d) the actual solution and the solution up to $O(\epsilon)$.

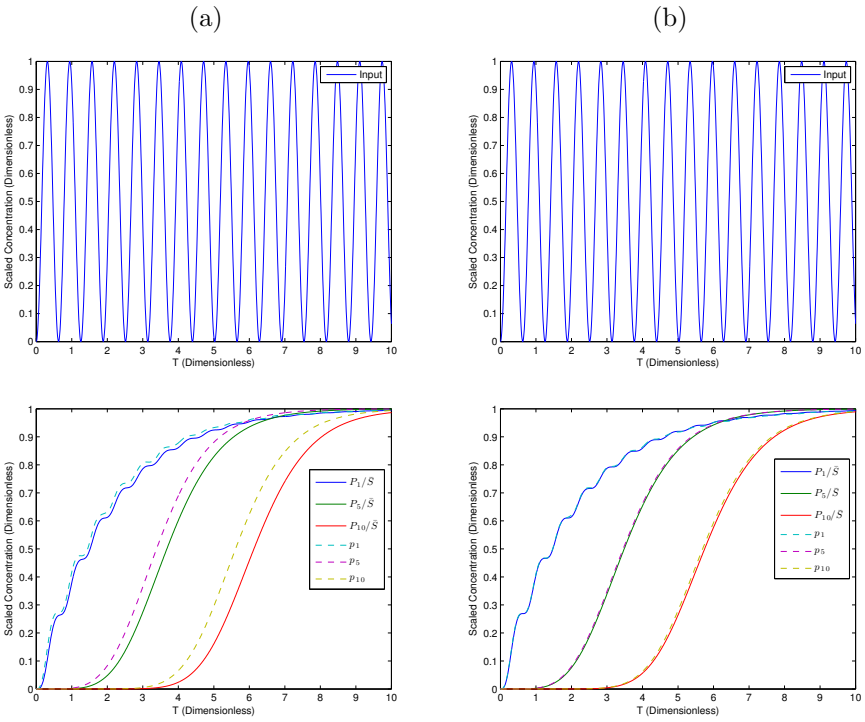


Figure 9: Plots demonstrating the accuracy of approximating an enzymatic cascade.

In column (a), the scaled input function and outputs for various $n$-layered cascades are plotted. $\epsilon = 0.1$ for the first column. In column (b), the same plots are displayed, except with $\epsilon = 0.01$.